

Pendulum with a square-wave modulated length

Eugene I. Butikov

St. Petersburg State University, St. Petersburg, Russia

Abstract

Parametric excitation of a rigid planar pendulum caused by a square-wave modulation of its length is investigated both analytically and with the help of computer simulations. The threshold and other characteristics of parametric resonance are found and discussed in detail. The role of nonlinear properties of the pendulum in restricting the resonant swinging is emphasized. The boundaries of parametric instability ranges are determined as functions of the modulation depth and the quality factor. Stationary oscillations at these boundaries and at the threshold conditions are investigated. The feedback providing active optimal control of pumping and damping is analyzed. Phase locking between the drive and the pendulum at large amplitudes and the phenomenon of parametric autoresonance are discussed.

Keywords: parametric resonance, optimal control, phase locking, autoresonance, bifurcations, instability ranges

1. Introduction: the investigated physical system

Periodic excitation of a physical system is called *parametric forcing* if it is realized by variation of some parameter that characterizes the system. In particular, a pendulum can be excited parametrically by a given vertical motion of its suspension point. In the frame of reference associated with the pivot, such forcing of the pendulum is equivalent to periodic modulation of the gravitational field. This apparently simple physical system exhibits a surprisingly vast variety of possible regular and chaotic motions. Hundreds of texts and papers are devoted to investigation of the pendulum with vertically oscillating pivot: see, for example, Refs. [1], [2] and references therein. A widely known curiosity in the behavior of an ordinary rigid planar pendulum whose pivot is forced to oscillate along the vertical line is the dynamic stabilization of its inverted position, occurring when the driving amplitude and frequency lie in certain intervals (see, for example, Refs. [2] – [5]).

Another familiar method of parametric excitation which we explore in this paper consists of a periodic variation of the length of the pendulum. In many textbooks and papers (see, for example, Refs. [6] – [10]) such a system is considered as a simple model of a playground swing. Indeed, the swing can be treated as a physical pendulum whose effective length changes periodically as the child squats at the extreme points, and straightens each time the swing passes through the equilibrium position. It is easy to illustrate this phenomenon of the swing pumping by the following simple experiment. Let a thread with a bob hanging on its end pass through a little ring fixed in a support. You can pull by some small distance the other end of the thread that you are holding in your hand each time the swinging bob passes through the middle position, and release the thread to its previous length each time the bob reaches its extreme positions. These periodic variations of the pendulum's length with the frequency twice the frequency of natural oscillation cause the amplitude to increase progressively.

A fascinating description of an exotic example illustrating this mode of parametric excitation can be found in Ref. [11], p. 27. In Spain, in the cathedral of a northern town Santiago de

Compostela, there is a famous *O Botafumeiro*, a very large incense burner suspended by a long rope, which can swing through a huge arc. The censer is pumped by periodically shortening and lengthening the rope as it is wound up and then down around the rollers supported high above the floor of the nave. The pumping action is carried out by a squad of priests, called *tiraboleiros* or ball swingers, each holding a rope that is a strand of the main rope that goes from the pendulum to the rollers and back down to near the floor. The *tiraboleiros* periodically pull on their respective ropes in response to orders from the chief verger of the cathedral. One of the more terrifying aspects of the pendulum's motion is the fact that the amplitude of its swing is very large, and it passes through the bottom of its arc with a high velocity, spewing smoke and flames.

In this paper we consider a pendulum with modulated length that can swing in the vertical plane in the uniform gravitational field. To allow arbitrarily large swinging and even full revolutions, we assume that the pendulum consists of a rigid massless rod (rather than a flexible string) with a massive small bob on its end. The effective length of the pendulum can be changed by shifting the bob along this rod. Periodic modulation of the effective length by such mass redistribution can cause, under certain conditions, a growth of initially small natural oscillations. This phenomenon is called parametric resonance.

2. The square-wave modulation of the pendulum length

In this paper we are concerned with a periodic square-wave (piecewise constant) modulation of the pendulum length. The square-wave modulation provides an alternative and may be more straightforward way to understand the underlying physics and to describe quantitatively the phenomenon of parametric resonance in comparison with a smooth (e.g., sinusoidal) modulation of the pendulum length [6] – [10]. A computer program [12] developed by the author simulates such a physical system and aids greatly in investigating the phenomenon.

In the case of the square-wave modulation, abrupt, almost instantaneous increments and decrements in the length of the pendulum occur sequentially, separated by equal time intervals. We denote these intervals by $T/2$, so that T equals the period of the length variation (the period of modulation). It is easy to understand how the square-wave modulation can produce considerable oscillation of the pendulum if the period and phase of modulation are chosen properly.

For example, suppose that the bob is shifted up (toward the axis) at an instant at which the pendulum passes through the lower equilibrium position, when its angular velocity reaches a maximum value. While the weight is moved radially, the angular momentum of the pendulum with respect to the pivot remains constant. Thus the resulting reduction in the moment of inertia is accompanied by an increment in the angular velocity, and the pendulum gets additional energy. The greater the angular velocity, the greater the increment in energy. This additional energy is supplied by the source that moves the bob along the rod.

On the other hand, if the bob is instantly moved down along the rod of the swinging pendulum, the angular velocity and the energy of the pendulum diminish. The decrease in energy is transferred back to the source. In order that increments in energy occur regularly and exceed the amounts of energy returned, i.e., in order that, as a whole, the modulation of the length regularly feeds the pendulum with energy, the period and phase of modulation must satisfy certain conditions.

In particular, the greatest growth of the amplitude occurs if effective length of the pendulum is reduced each time the pendulum crosses the equilibrium position, and is increased back at greatest elongations, when the angular velocity is almost zero. Therefore this radial displacement of the bob into its former position causes nearly no decrement in the kinetic energy. The resonant growth of the amplitude occurs if two cycles of modulation are executed during one

period of natural oscillations. This is the principal parametric resonance. The time history of such oscillations for the case of a very weak friction ($Q = 1500$) is shown in Fig. 1 together with the square-wave variation of the pendulum length.

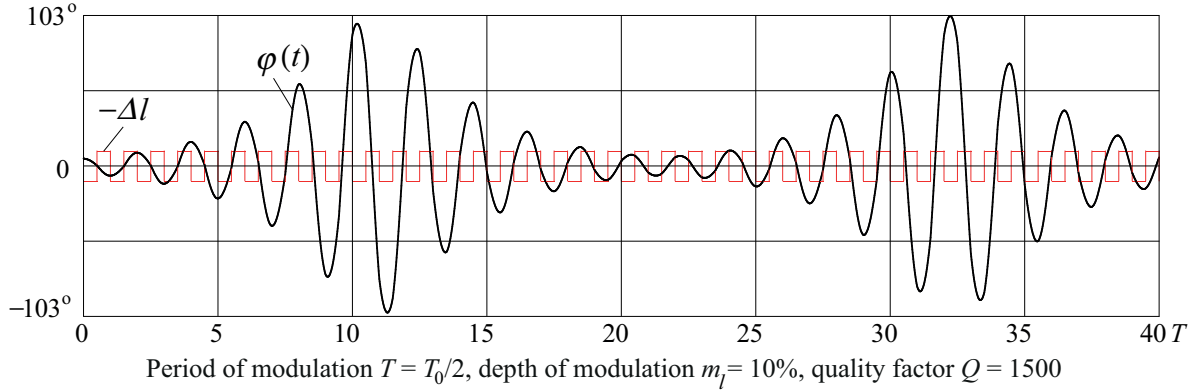


Figure 1: Initial exponential growth of the amplitude of oscillations at parametric resonance of the first order ($n = 1$) under the square-wave modulation, followed by beats.

In a real system the growth of the amplitude at parametric resonance is restricted by nonlinear effects. In a nonlinear system like the pendulum, the natural period depends on the amplitude of oscillations. As the amplitude grows, the natural period of the pendulum becomes longer. However, in the accepted model the drive period (period of modulation) remains constant. If conditions for parametric excitation are fulfilled at small oscillations and the amplitude is growing, the conditions of resonance become violated at large amplitudes — the drive slips out of resonance. The drive will then drift out of phase with the pendulum. The phase relationships between the modulation and oscillations of the pendulum change gradually to those favorable for the backward transfer of energy from the pendulum to the source of modulation. This causes gradual reduction of the amplitude. The natural period becomes shorter, and conditions for the growth of the amplitude restore. Oscillations of the pendulum acquire the character of beats, as shown in Fig. 1. Due to friction these transient beats gradually fade, and the amplitude tends to a finite constant value.

Details of the process of resonant growth followed by a nonlinear restriction of the amplitude for parametrically excited pendulum ($T = T_0/2$) with considerable values of the modulation depth and friction ($m_l = 15\%$, $Q = 5.0$) are shown in Fig. 2. The vertical segments of the phase trajectory and of the $\dot{\varphi}(t)$ graph correspond to instantaneous increments and decrements of the angular velocity $\dot{\varphi}$ at the instants at which the bob is shifted up and down respectively. The curved portions of the phase trajectory that spiral in toward the origin correspond to damped natural motions of the pendulum between the jumps of the bob. The initially fast growth of the amplitude (described by the expanding part of the phase trajectory) gradually slows down, because the natural period becomes longer. After reaching the maximum value of 78.3° , the amplitude alternatively decreases and increases within a small range approaching slowly its final value of about 74° . The initially unwinding spiral of the phase trajectory simultaneously approaches the closed limit cycle, whose characteristic shape can be seen in the left part of Fig. 2.

It is evident that the energy of the pendulum is increased not only when two full cycles of variation in the parameter occur during one natural period of oscillation, but also when two cycles occur during three, five or any odd number of natural periods (resonances of odd orders). We shall see later that the delivery of energy, though less efficient, is also possible if two cycles of modulation occur during an even number of natural periods (resonances of even orders).

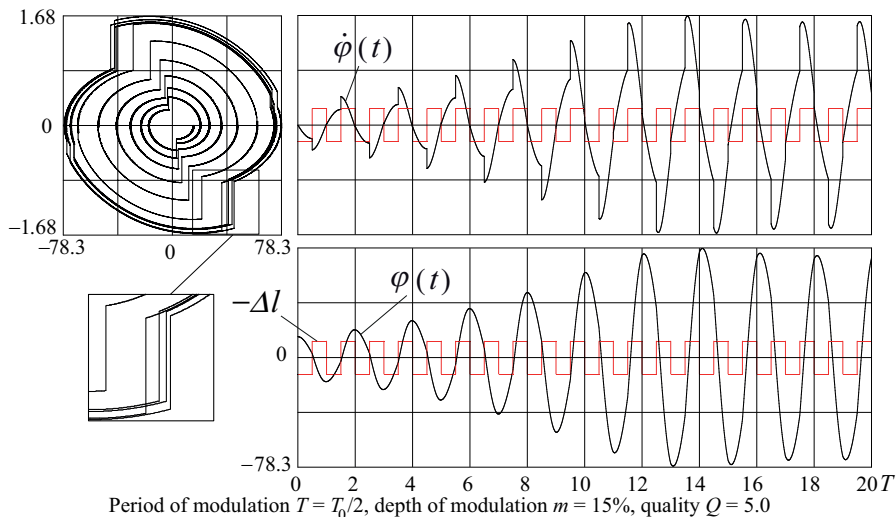


Figure 2: The phase diagram ($\varphi - \dot{\varphi}$ plane, left) and time-dependent graphs (right) of angular velocity $\dot{\varphi}(t)$ and angle $\varphi(t)$ for the process of resonant growth followed by nonlinear restriction of the amplitude. The square-wave modulation of the pendulum length is also shown (up and down positions of the pendulum bob).

3. The threshold of parametric excitation

There are several important differences that distinguish parametric resonance from the ordinary resonance caused by an external force exerted directly on the system. Variations of the length cannot take a resting pendulum out of equilibrium: in contrast to the direct forcing, parametric excitation can occur only if (even small) natural oscillations already exist. Parametric resonance is possible when one of the following conditions for the frequency ω (or for the period T) of a parameter modulation is fulfilled:

$$\omega = \omega_n = \frac{2\omega_0}{n}, \quad T = T_n = \frac{nT_0}{2}, \quad n = 1, 2, \dots \quad (1)$$

Parametric resonance is possible not only at the frequencies ω_n given in Eq. (1), but also in ranges of frequencies ω lying on either side of the values ω_n (in the ranges of instability). These intervals become wider as the depth of modulation is increased.

An important distinction between parametric excitation and forced oscillations is related to the dependence of the growth of energy on the energy already stored in the system. While for a direct forced excitation the increment in energy during one period is proportional to the amplitude of oscillations, i.e., to the square root of the energy, at parametric resonance the increment in energy is proportional to the energy itself, stored in the system.

Energy losses caused by friction are also proportional to the energy already stored. In the case of direct forced excitation, energy losses restrict the growth of the amplitude because these losses grow with the energy faster than does the investment in energy arising from the work done by the external force. In the case of parametric resonance, both the investment in energy caused by the modulation of a parameter and the frictional losses are proportional to the energy stored, and so their ratio does not depend on the amplitude. Therefore, parametric resonance is possible only when a *threshold* is exceeded, that is, when the increment in energy during a period (caused by the parameter variation) is larger than the amount of energy dissipated during the same time. The critical (threshold) value of the modulation depth depends on friction. However, if the threshold is exceeded, the frictional losses of energy cannot restrict the growth of the amplitude. With friction, stationary oscillations of a finite amplitude eventually establish due to nonlinear properties of the pendulum.

We can use arguments employing the conservation laws to evaluate the modulation depth which corresponds to the threshold of the principal parametric resonance. Let the changes in the length l of the pendulum occur between $l_1 = l_0(1 + m_l)$ and $l_2 = l_0(1 - m_l)$, where m_l is the dimensionless *depth of modulation* (or modulation index). To calculate the change in total energy of the pendulum during a period, we should not worry about the potential energy. Indeed, after a period the pendulum occurs again in the vertical position with the bob at the same height, hence after a period its potential energy is the same. Thus we should calculate only the change in kinetic energy.

Next we calculate the fractional increment in energy $\Delta E/E$ during one cycle of modulation, namely, between two consecutive passages through the equilibrium position in opposite directions. At the first passage, the energy E_1 equals $v_1^2/2$ per unit mass of the bob, where v_1 is the bob's velocity. At this time moment the bob is shifted up, so the length of the pendulum changes from $l_0(1 + m_l)$ to $l_0(1 - m_l)$. During abrupt radial displacements of the bob along the pendulum rod, the angular momentum $L = J\dot{\varphi} = Ml^2\dot{\varphi}$ is conserved (M is mass of the bob, $J = Ml^2$ is the moment of inertia about the pivot). Therefore the angular velocity changes at this moment from $\dot{\varphi}_1$ to $(1 + m_l)^2/(1 - m_l)^2\dot{\varphi}_1$. This means that the linear velocity v of the bob changes from $v_1 = l_0(1 + m_l)\dot{\varphi}_1$ to $l_0(1 + m_l)/(1 - m_l)v_1$. Then the pendulum moves from the vertical $\varphi = 0$ up to the maximum deflection φ_m , whose value can be calculated using the energy conservation:

$$\frac{1}{2}v_1^2 \left(\frac{1 + m_l}{1 - m_l} \right)^2 = g l_0(1 - m_l)(1 - \cos \varphi_m). \quad (2)$$

When the frequency and phase of the modulation have those values which are favorable for the most effective delivery of energy to the pendulum, the abrupt backward displacement of the bob toward the end of the rod occurs at the instant when the pendulum attains its greatest deflection (more precisely, when the pendulum is very near it). At this instant the angular velocity of the pendulum is almost zero. Hence this action produces no change in the kinetic energy. At this time moment the bob is shifted down, and the length of the pendulum becomes $l_0(1 + m_l)$. The pendulum starts its backward motion with zero velocity. Velocity v_2 in the equilibrium position which is gained during this motion, again can be calculated, like in Eq. (2), on the basis of energy conservation:

$$\frac{1}{2}v_2^2 = g l_0(1 + m_l)(1 - \cos \varphi_m). \quad (3)$$

From Eqs.(2)–(3) we find:

$$v_2^2 = v_1^2 \left(\frac{1 + m_l}{1 - m_l} \right)^3, \quad E_2 = E_1 \left(\frac{1 + m_l}{1 - m_l} \right)^3, \quad (4)$$

where $E_2 = v_2^2/2$ is the kinetic energy (per unit mass) after a period T of modulation. Hence

$$\frac{\Delta E}{E} = \frac{E_2}{E_1} - 1 = \left(\frac{1 + m_l}{1 - m_l} \right)^3 - 1 \approx 6 m_l. \quad (5)$$

The last approximate expression in Eq. (5) is valid for small values of the modulation depth $m_l \ll 1$. That is, the fractional increment of total energy $\Delta E/E$ during one period T of modulation approximately equals $6m_l$. The sequence of energy values E_n at consecutive passages through the equilibrium position forms a geometric progression. A process in which the increment in energy ΔE during a period is proportional to the energy E stored ($dE/dt \approx 6m_l E/T$) is characterized on average by the exponential growth of the energy with time:

$$E(t) = E_0 \exp\left(\frac{6m_l}{T} t\right) = E_0 \exp(\alpha t). \quad (6)$$

In this case the index of growth α is proportional to the depth of modulation m_l of the pendulum length: $\alpha = 6m_l/T$. When the modulation is exactly tuned to the principal resonance ($T = T_0/2$), the decrease of energy is caused almost only by friction. Dissipation of energy due to viscous friction during an integer number of natural half-cycles (for $t = nT = nT_0/2$) is described by the following expression:

$$E(t) = E_0 \exp(-2\gamma t), \quad (7)$$

where γ is the damping constant for the amplitude. Comparing equations (6) and (7), we obtain the following estimate for the threshold (minimal) value $(m_l)_{\min}$ of the depth of modulation corresponding to the excitation of the principal parametric resonance:

$$(m_l)_{\min} = \frac{1}{3}\gamma T = \frac{1}{6}\gamma T_0 = \frac{\pi}{6Q}. \quad (8)$$

Here we introduced the dimensionless quality factor $Q = \omega_0/(2\gamma)$ to characterize the strength of viscous friction in the system.

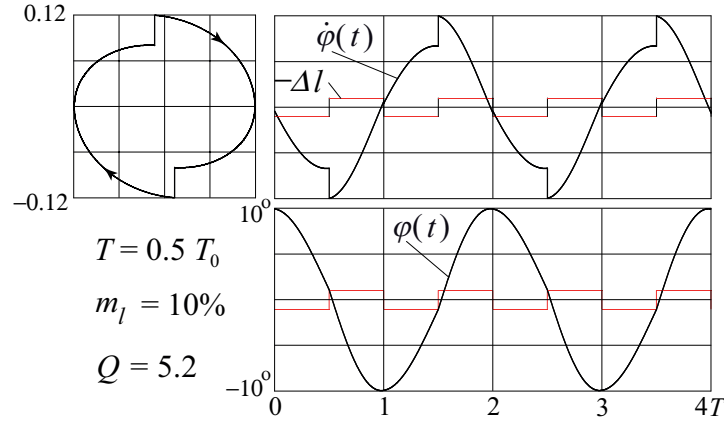


Figure 3: The phase trajectory (left) and the time-dependent graphs of stationary oscillations (right) at the threshold condition $m_l \approx \pi/(6Q)$ for $T = T_0/2$.

The phase trajectory and the plots of time dependence of the angle and angular velocity of parametric oscillations of a small amplitude occurring at the threshold conditions, Eq. (8), are shown in Fig. 3. We can see on the graphs and the phase trajectory only abrupt increments in the magnitude of the angular velocity occurring twice during the period of oscillation (when the bob is shifted upward). The downward shifts of the bob occur at instants when the angular velocity is almost zero. Therefore the corresponding decrements in velocity are too small to be visible on the graphs. This mode of steady oscillations (which have a constant amplitude in spite of the dissipation of energy) is called *parametric regeneration*. Computer simulations show that regime of parametric regeneration is stable with respect to small variations in initial conditions: at different initial conditions the phase trajectory and graphs acquire after a while the same characteristic shape. However, this regime is unstable with respect to variations of the pendulum parameters. If the friction is slightly greater or the depth of modulation slightly smaller than Eq. (8) requires, oscillations gradually damp in spite of the modulation. Otherwise, the amplitude grows.

For the third resonance ($T = 3T_0/2$) the threshold value of the depth of modulation is three times greater than its value for the principal resonance: $(m_l)_{\min} = \pi/(2Q)$. In this instance two cycles of the parametric variation occur during three full periods of natural oscillations.

Radial displacements of the pendulum bob again happen at the time moments most favorable for pumping the pendulum — up at the equilibrium position, and down at the extreme positions. The same investment in energy occurs during an interval that is three times longer than the interval for the principal resonance.

When the depth of modulation exceeds the threshold value, the energy of initially small oscillations during the first stage increases exponentially with time. For the principal parametric resonance this initial growth is shown in Fig. 4. The growth of the energy again is described by

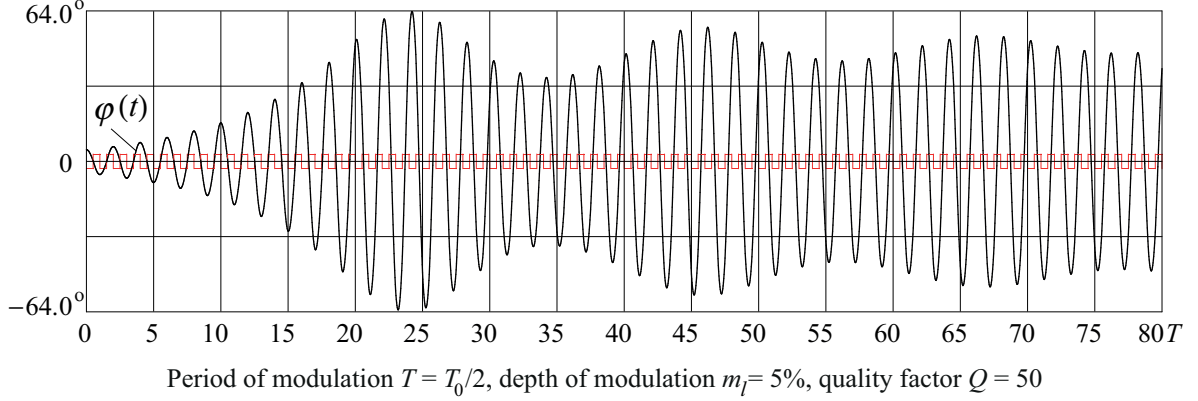


Figure 4: Gradually fading beats of the amplitude of oscillations at parametric resonance of the first order ($n = 1$).

Eq. (6). However, now the index of growth α is determined by the amount by which the energy delivered through parametric modulation exceeds the simultaneous losses of energy caused by friction: $\alpha = 6m_l/T - 2\gamma$. If the swing is small enough, the energy is proportional to the square of the amplitude. Hence the amplitude of parametrically excited oscillations initially also increases exponentially with time: $a(t) = a_0 \exp(\beta t)$. The index β in the growth of amplitude is one half the index of the growth in energy. For the principal resonance, when the investment in energy occurs twice during one natural period of oscillation, we have $\beta = 3m_l/T - \gamma = 6m_l/T_0 - \gamma = 3m_l\omega_0/\pi - \gamma$.

If the threshold is exceeded, the amplitude grows, conditions of resonance violate, and this causes a gradual reduction of the amplitude. At small amplitudes the natural period becomes shorter, conditions of resonance restore, so that oscillations of the pendulum acquire the character of beats. Due to friction, these transient beats gradually fade, and eventually steady-state oscillations of a finite amplitude establish (Fig. 4). We note again that the growth of amplitude is restricted by nonlinear properties of the pendulum, namely, by the dependence of the natural period T_0 on the amplitude. For small and moderate values of the amplitude φ_m this dependence is approximately given by $T_0(\varphi_m) \approx T_{\text{small}}(1 + \varphi_m^2/16)$, where T_{small} is the period of infinitely small natural oscillations. In contrast with the ordinary resonance caused by direct periodic forcing in a linear isochronous system, friction alone cannot restrict the growth of the amplitude at parametric resonance. In an idealized linear system the amplitude of parametric oscillations over the threshold grows indefinitely (Refs. [14] – [15]).

4. Feedback, parametric autoresonance, bifurcations, multistability

In the above analysis we assumed that the period T of modulation remains the same as the amplitude increases. At exact tuning to the principal resonance this period equals $T_0/2$, where T_0 is the period of small natural oscillations. When we apply the model of the pendulum with modulated length for explaining the pumping of a playground swing, we should take into

account that the child on the swing may notice the lengthening of the natural period as the amplitude increases, and can react correspondingly, increasing the period of pumping to stay in phase with the swing. This intuitive reaction may be considered as a kind of feedback loop: the child determines the time instants to squat and to stand depending on the actual position of the swing. We can include this feedback loop in our model by requiring that instantaneous upward shifts of the bob of the pendulum occur exactly at the time moments, at which the pendulum crosses the equilibrium position, and that backward shifts of the bob to the end of the rod occur exactly at extreme positions of the pendulum. Such manipulations provide the optimal active control for the most effective and rapid pumping.

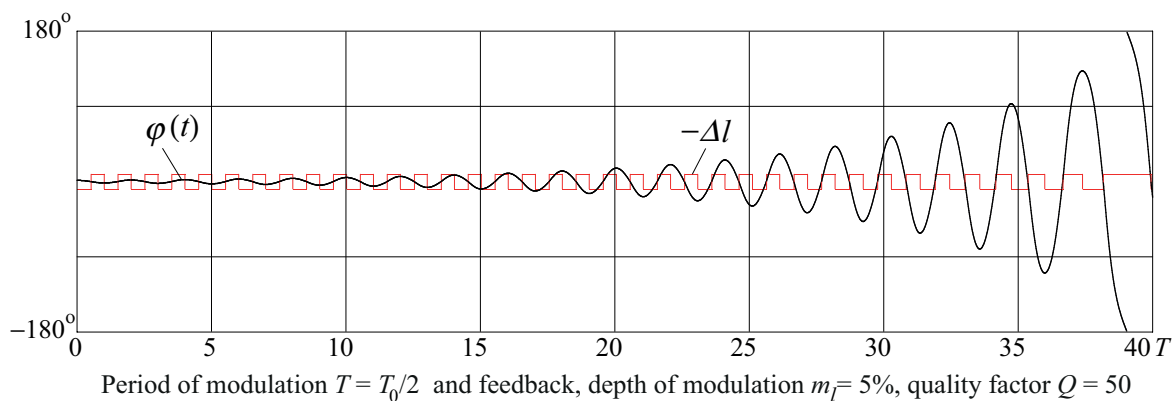


Figure 5: Parametric pumping of the pendulum with the usage of a feedback loop that provides the most effective delivery of energy to the pendulum.

Figure 5 shows the graph of progressively growing oscillations occurring under this optimal control with a feedback. Initially the period of modulation T satisfies conditions of the principal parametric resonance at small swing ($T = T_0/2$). We note how the period T of the square-wave modulation increases with the amplitude due to the feedback. After the amplitude reaches 180° , the pendulum executes full revolutions.

Certainly, the priests that pump *O Botafumeiro* also use the feedback (maybe intuitively) for controlling the pendulum behavior. They increase gradually the period of modulation as the amplitude grows, and then probably reduce the depth of modulation to the level, sufficient to compensate for frictional losses and to maintain the desirable swing.

The strategy of optimal active control for the most rapid damping of existing oscillations on the basis of feedback consists in reversing the phase of modulation. Namely, the length of the pendulum must be increased at moments of crossing the equilibrium position, and the length must be reduced at extreme positions.

Is it possible to excite large oscillations of the pendulum at a small excess of the drive over the threshold without the feedback, that is, without appropriately adjusting the period and phase of modulation as the amplitude grows? It occurs that under certain conditions a spontaneous phase locking between the drive and the pendulum motion becomes possible: the pendulum can automatically adjust its amplitude to stay matched with the drive. By sweeping the drive period appropriately, we can control the amplitude of the pendulum. This phenomenon is called *parametric autoresonance*. Autoresonance allows us to both excite and control a large resonant response in nonlinear systems by a small forcing.

We can start pumping the pendulum by modulating its length with period $T = T_0/2$, which corresponds to resonant condition at an infinitely small swing. Then, in the process of oscillations, we slowly increase the period of modulation. This can be done in small steps. After

each increment of the period we wait for a while so that transients almost fade away. During this time the amplitude increases just to the amount which provides matching of an increased natural period of the pendulum with the new period of modulation. Thus in each step of this sweeping the pendulum remains locked in phase with the drive.

To illustrate the phenomenon of parametric autoresonance in a computer simulation (Fig. 6), we choose the following values for the pendulum parameters: depth of modulation 5%, quality factor $Q = 20$. When the period of modulation is gradually increased from $T = 0.5T_0$ up to $T = 0.9T_0$, the pendulum swings with an amplitude of 153° . At $T = 0.90T_0$ a bifurcation of symmetry breaking occurs: the pendulum swings to one side through an angle of 161° , while its excursion to the other side is only 146° . This asymmetry in the swing increases up to $T = 0.913T_0$, when a bifurcation of period doubling occurs: during two cycles of modulation the pendulum executes one asymmetric oscillation between the values 161.39° and 146.88° , while during the next two cycles the pendulum swings between 161.49° and 144.25° . Then the process repeats. Thus one period of the pendulum motion covers now four periods of excitation. These oscillations are illustrated in Fig. 6. We note that the closed phase trajectory is formed by two nearby almost merging loops. Such asymmetric regimes exist (for the same values of m_l and Q) in pairs, whose phase orbits are mirror images of one another.

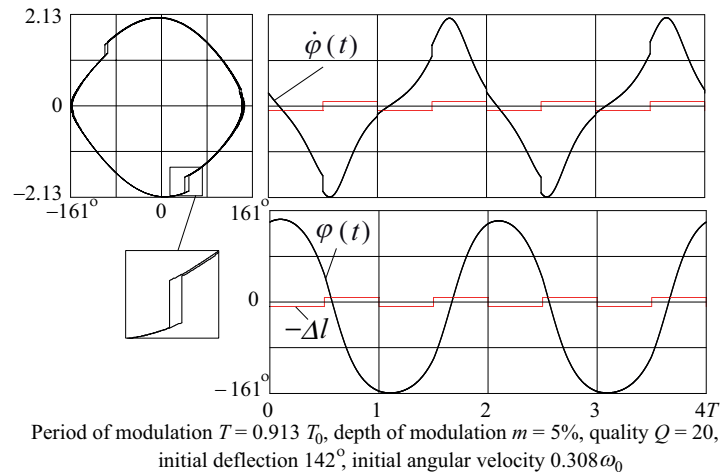


Figure 6: Bifurcation of period doubling in parametric autoresonance.

Further increasing of the drive period by tiny steps causes a whole condensing cascade of nearby period doubling bifurcations, which ends at $T = 0.9148T_0$ by a crisis: oscillations of the pendulum become unstable, finally it turns over the upper equilibrium, and then, after long irregular transient oscillations with gradually diminishing amplitude, eventually comes to rest in the downward vertical position.

Stationary parametric oscillations of the pendulum with large amplitude, locked in phase with the drive and occurring at a small or moderate modulation (like those described above and shown in Fig. 6), can be excited not only by slowly sweeping the drive period, but also by appropriate initial conditions. The system eventually comes to a certain periodic regime (limit cycle, or attractor), if initial conditions are chosen within the basin of attraction of this regime. In nonlinear systems different periodic regimes may coexist at the same values of parameters. This property is called multistability.

An example of multistability is shown in Fig. 7. Curve 1 (upper side of Fig. 7) describes stationary periodic oscillations of the pendulum with a finite amplitude corresponding to the principal parametric resonance. One period of these oscillations covers two cycles of excitation.

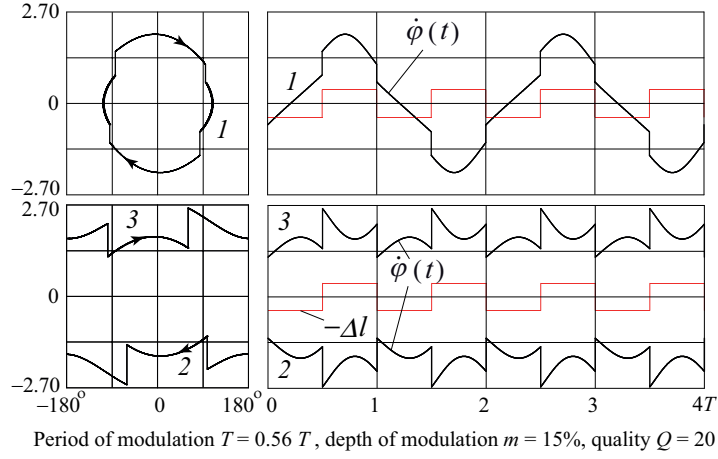


Figure 7: Stationary periodic oscillations and rotations, occurring at the same values of the system parameters.

Curves 2 and 3 (lower side of Fig. 7) correspond to period-1 unidirectional rotations of the pendulum in clockwise and counterclockwise directions respectively. The pendulum makes one revolution during each period of modulation. One more attractor is represented by a single point at the origin of the phase plane, which describes the state of rest of the pendulum in the downward vertical position. Each of these different stationary modes, coexisting at the same values of all parameters of the pendulum and the drive, is characterized by a certain basin of attraction in the phase plane of initial states.

5. Governing equation for parametric oscillations and the mean natural period at large depth of modulation

Next we consider a more rigorous mathematical treatment of parametric resonance under square-wave modulation of the parameter. During the time intervals $(0, T/2)$ and $(T/2, T)$, the length of the pendulum is constant, and its motion can be considered as a free oscillation described by a corresponding differential equation. However, the coefficients in this equation are different for the adjacent time intervals $(0, T/2)$ and $(T/2, T)$:

$$\ddot{\varphi} + 2\gamma\dot{\varphi} + \omega_1^2 \sin \varphi = 0, \quad \omega_1 = \frac{\omega_0}{\sqrt{1+m}} \quad \text{for } 0 < t < T/2, \quad (9)$$

$$\ddot{\varphi} + 2\gamma\dot{\varphi} + \omega_2^2 \sin \varphi = 0, \quad \omega_2 = \frac{\omega_0}{\sqrt{1-m}} \quad \text{for } -T/2 < t < 0. \quad (10)$$

Here $\omega_0 = \sqrt{g/l_0}$ is the natural frequency of small oscillations for the pendulum with mean length l_0 , and γ is the damping constant characterizing the strength of viscous friction. For a slow pendulum traveling in air, the linear dependence of drag on velocity is a reasonable approximation. When damping is caused by the drag force exerted on the pendulum bob, and this force is proportional to the linear velocity of the bob, the frictional torque about the pivot is proportional to l^2 . Since the moment of inertia is also proportional to l^2 , the damping constant γ in this model remains the same when the length of the pendulum changes, that is, its values in Eqs. (9) and (10) are equal.

At each instant $t_n = nT/2$ ($n = 1, 2, \dots$) of an abrupt change in the length of the pendulum, we must make a transition from one of these equations (9)–(10) to the other. During each half-period $T/2$ the motion of the pendulum is a segment of some natural oscillation. An analytical investigation of parametric excitation can be carried out by fitting to one another known solutions to equations (9)–(10) for consecutive adjacent time intervals.

The initial conditions for each subsequent time interval are chosen according to the physical model in the following way. Each initial value of the angular displacement φ equals the value $\varphi(t)$ reached by the oscillator at the end of the preceding time interval. The initial value of the angular velocity $\dot{\varphi}$ is related to the angular velocity at the end of the preceding time interval by the law of conservation of the angular momentum:

$$(1 + m_l)^2 \dot{\varphi}_1 = (1 - m_l)^2 \dot{\varphi}_2. \quad (11)$$

In Eq. (11) $\dot{\varphi}_1$ is the angular velocity at the end of the preceding time interval, when the moment of inertia of the pendulum has the value $J_1 = J_0(1 + m_l)^2$, and $\dot{\varphi}_2$ is the initial value for the following time interval, during which the moment of inertia equals $J_2 = J_0(1 - m_l)^2$. The change in the angular velocity at an abrupt variation of the inertia moment from the value J_2 to J_1 can be found in the same way.

We may use here the conservation of angular momentum, as expressed in Eq. (11), because at sufficiently rapid displacement of the bob along the rod of the pendulum, the influence of the torque produced by the force of gravity is negligible. In other words, we can assume the pendulum to be freely rotating about its axis. This assumption is valid provided the duration of the displacement of the bob constitutes a small portion of the natural period.

Considering conditions for which equations (9)–(10) yield solutions with increasing amplitudes, we can determine the ranges of frequency ω near the values $\omega_n = 2\omega_0/n$, within which the state of rest is unstable for a given modulation depth m_l . In these ranges of parametric instability an arbitrarily small deflection from equilibrium is sufficient for the progressive growth of small initial oscillations.

The threshold for the parametric excitation of the pendulum is determined above for the resonant situations in which two cycles of the parametric modulation occur during one natural period or during three natural periods of oscillation. The estimate obtained, Eq. (8), is valid for small values of the modulation depth m_l of the pendulum length.

For large values of the modulation depth m_l , the notion of a natural period needs a more precise definition. Let $T_0 = 2\pi/\omega_0 = 2\pi\sqrt{l_0/g}$ be the period of oscillation of the pendulum when its massive bob is fixed in the middle position, for which the effective length equals l_0 . The period is somewhat longer when the weight is moved further from the axis: $T_1 = T_0\sqrt{1 + m_l} \approx T_0(1 + m_l/2)$. The period is shorter when the weight is moved closer to the axis: $T_2 = T_0\sqrt{1 - m_l} \approx T_0(1 - m_l/2)$.

It is convenient to define the natural average period T_{av} not as the arithmetic mean $\frac{1}{2}(T_1 + T_2)$, but rather as the period that corresponds to the arithmetic mean frequency $\omega_{\text{av}} = \frac{1}{2}(\omega_1 + \omega_2)$, where $\omega_1 = 2\pi/T_1$ and $\omega_2 = 2\pi/T_2$. So we define T_{av} by the relation:

$$T_{\text{av}} = \frac{2\pi}{\omega_{\text{av}}} = \frac{2T_1T_2}{(T_1 + T_2)}. \quad (12)$$

Indeed, the period T of the parametric modulation which is exactly tuned to any of the parametric resonances is determined not only by the order n of the resonance, but also by the depth of modulation m_l . In order to satisfy the resonant conditions, the increment in the phase of natural oscillations during one cycle of modulation must be equal to $\pi, 2\pi, 3\pi, \dots, n\pi, \dots$. During the first half-cycle the phase of oscillation increases by $\omega_1 T/2$, and during the second half-cycle — by $\omega_2 T/2$. Consequently, instead of the approximate condition expressed by Eq. (1), we obtain:

$$\frac{\omega_1 + \omega_2}{2} T = n\pi, \quad \text{or} \quad T = T_n = n \frac{\pi}{\omega_{\text{av}}} = n \frac{T_{\text{av}}}{2}. \quad (13)$$

Thus, for a parametric resonance of some definite order n , the condition for exact tuning can be expressed in terms of the two natural periods, T_1 and T_2 . This condition is $T = nT_{\text{av}}/2$, where

T_{av} is defined by Eq. (12). For small and moderate values of m_l it is possible to use approximate expressions for the average natural frequency and period:

$$\omega_{\text{av}} = \frac{\omega_0}{2} \left(\frac{1}{\sqrt{1+m_l}} + \frac{1}{\sqrt{1-m_l}} \right) \approx \omega_0 \left(1 + \frac{3}{8}m_l^2 \right), \quad T_{\text{av}} \approx T_0 \left(1 - \frac{3}{8}m_l^2 \right). \quad (14)$$

The difference between T_{av} and T_0 reveals itself in terms proportional to the square of the depth of modulation m_l .

6. Frequency ranges for parametric resonances of odd orders

To find the boundaries of the frequency ranges of parametric instability surrounding the resonant values $T = T_{\text{av}}/2$, $T = T_{\text{av}}$, $T = 3T_{\text{av}}/2$, \dots , we can consider stationary oscillations of indefinitely small amplitude that occur when the period of modulation T corresponds to one of the boundaries. These periodic stationary oscillations can be represented as an alternation of natural oscillations with the periods T_1 and T_2 .

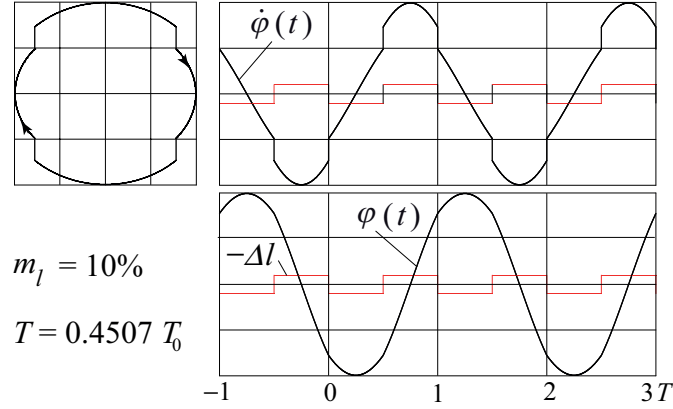


Figure 8: Phase trajectory and time-dependent graphs of stationary parametric oscillations at the lower boundary of the principal interval of instability (near $T = T_{\text{av}}/2$).

6.1. Main interval of parametric instability

We examine first the vicinity of the principal resonance occurring at $T = T_{\text{av}}/2$. Suppose that the period T of the parametric square-wave modulation is a little shorter than the resonant value $T = T_{\text{av}}/2$, so that T corresponds to the left boundary of the interval of instability. In this case a little less than a quarter of the mean natural period T_{av} elapses between consecutive abrupt increases and decreases of the pendulum length. Stationary regime with a constant swing in the absence of friction can be realized only if the abrupt increments and decrements of the angular velocity are equal in magnitude. The graphs of the angle $\varphi(t)$ and angular velocity $\dot{\varphi}(t)$ for this periodic stationary process have the characteristic symmetric patterns shown in Fig. 8. The segments of the graphs of free oscillations (which occur within time intervals during which the length of the pendulum is constant) are alternating parts of sine or cosine curves with the periods T_1 and T_2 . These segments are symmetrically truncated on both sides.

To find conditions at which such stationary oscillations take place, we can write the expressions for $\varphi(t)$ and $\dot{\varphi}(t)$ during the adjacent intervals in which the oscillator executes natural oscillations, and then fit these expressions to one another at the boundaries. Such fitting must provide a periodic stationary process.

We let the origin of time, $t = 0$, be the instant when the bob is shifted downward. The angular velocity is abruptly decreased in magnitude at this instant (see Fig. 8). Then during the interval $(0, T/2)$ the graph describes a natural oscillation with the frequency $\omega_1 = \omega_0/\sqrt{1+m}$. Since the graph is symmetric with respect to time moment $T/4$, we can write the corresponding time dependencies of $\varphi(t)$ and $\dot{\varphi}(t)$ in the following form:

$$\varphi_1(t) = -A_1 \cos \omega_1(t - T/4), \quad \dot{\varphi}_1(t) = A_1 \omega_1 \sin \omega_1(t - T/4), \quad 0 < t < T/2. \quad (15)$$

Similarly, during the interval $(-T/2, 0)$ the graph in Fig. 8 is a segment of natural oscillation with the frequency $\omega_2 = \omega_0/\sqrt{1-m}$:

$$\varphi_2(t) = -A_2 \sin \omega_2(t + T/4), \quad \dot{\varphi}_2(t) = -A_2 \omega_2 \cos \omega_2(t + T/4), \quad -T/2 < t < 0. \quad (16)$$

To determine the values of constants A_1 and A_2 , we use the conditions that must be satisfied when the segments of the graph are joined together, and take into account the periodicity of the stationary process. At $t = 0$ the angle of deflection is the same for both φ_1 and φ_2 , that is, $\varphi_1(0) = \varphi_2(0)$. The angular velocity at $t = 0$ undergoes a sudden change, which follows from the conservation of angular momentum: $(1+m_l)^2 \dot{\varphi}_1(0) = (1-m_l)^2 \dot{\varphi}_2(0)$, see Eq. (11). From these conditions of fitting the graphs we find the following equations for A_1 and A_2 :

$$A_1 \cos(\omega_1 T/4) = A_2 \sin(\omega_2 T/4). \quad (17)$$

$$A_1(1+m_l)^2 \omega_1 \sin(\omega_1 T/4) = A_2(1-m_l)^2 \omega_2 \cos(\omega_2 T/4). \quad (18)$$

These homogeneous equations (17)–(18) for A_1 and A_2 are compatible only if the following condition is fulfilled:

$$(1+m_l)^2 \omega_1 \sin(\omega_1 T/4) \sin(\omega_2 T/4) = (1-m_l)^2 \omega_2 \cos(\omega_1 T/4) \cos(\omega_2 T/4). \quad (19)$$

This is the equation that determines period T of modulation (for a given value m_l of the depth of modulation) which corresponds to the left boundary of the interval of parametric instability. Next we rearrange Eq. (19) to the following form which is convenient for obtaining its numeric solution for the unknown variable T :

$$(q+1) \cos(\omega_{\text{av}} T/2) = (q-1) \cos(\Delta\omega T/4), \quad (20)$$

where $\omega_{\text{av}} = (\omega_1 + \omega_2)/2$, and $\Delta\omega = \omega_2 - \omega_1$. In Eq. (20) we have introduced a dimensionless quantity q which depends on the depth of modulation m_l :

$$q = \left(\frac{1+m_l}{1-m_l} \right)^{3/2}. \quad (21)$$

To find the left boundary T_- of the instability interval which contains the principal parametric resonance, we search for a solution T to Eq. (20) in the vicinity of $T = T_0/2$. We replace T in the argument of the cosine on the left-hand side of Eq. (20) by $T_{\text{av}}/2 + \Delta T$. Since $\omega_{\text{av}} T_{\text{av}} = 2\pi$, we can write the cosine as $-\sin(\omega_{\text{av}} \Delta T/2)$. Then Eq. (20) becomes:

$$\sin(\omega_{\text{av}} \Delta T/2) = -\frac{q-1}{q+1} \cos \frac{\Delta\omega(T_{\text{av}}/2 + \Delta T)}{4}. \quad (22)$$

This equation for the unknown quantity ΔT can be solved numerically by iteration. We start with $\Delta T = 0$ as an approximation of the zeroth order, substituting it into the right-hand side of Eq. (22). Then the left-hand side of Eq. (22) gives us the value of ΔT to the first order. We

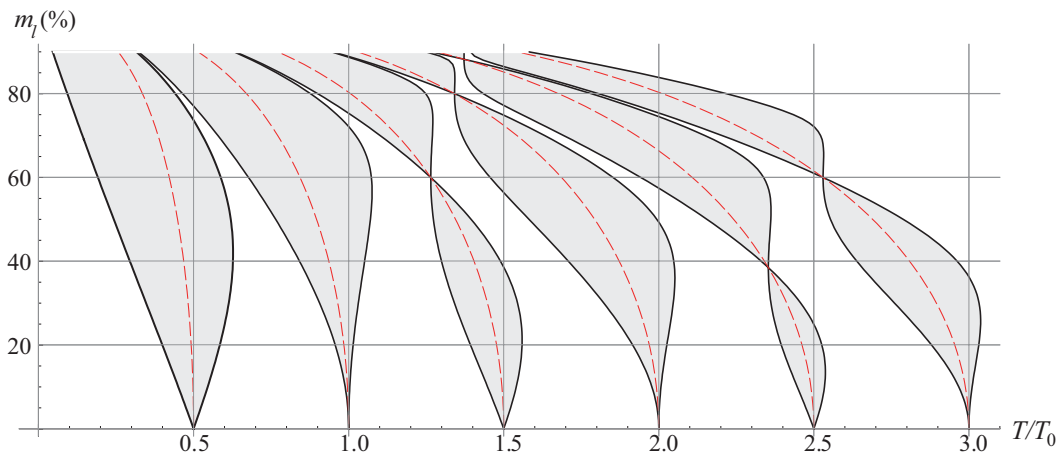


Figure 9: Intervals of parametric instability at square-wave modulation of the pendulum length in the absence of friction.

substitute this first-order value into the right-hand side of Eq. (22), and on the left-hand side we obtain ΔT to the second order. This procedure is iterated until a self-consistent value of ΔT for the left boundary is obtained. Performing such calculations for various values of the modulation depth m_l , we obtain the whole left boundary $T_-(m_l)$ for the first interval of parametric instability. Below we explain how the right boundary of this interval can be calculated, as well as the boundaries of other intervals.

The intervals of instability in the plane $T - m_l$ for the first six parametric resonances, calculated numerically with the help of the above described procedure, are shown in Fig. 9. This is an analog of the Ince-Strutt diagram of parametric instability for a system which is described by Mathieu equation, say, for a pendulum with vertical oscillations of the suspension point.

To observe stationary oscillations that correspond to the left boundary of the instability interval (see Fig. 8) in the simulation, it is insufficient to choose for period T of modulation a self-consistent solution to Eq. (22) for a given value of modulation depth m_l . After period T is calculated, also the initial conditions should be chosen properly. This can be done on the basis of Eq.(15), according to which for an arbitrary initial displacement $\varphi(0)$ the initial angular velocity should have the value $\dot{\varphi}_1(0) = \omega_1 \tan(\omega_1 T/4) \varphi_1(0)$.

For the right boundary of the main interval of instability, the period T of the parametric square-wave modulation is a little longer than the resonant value $T = T_{av}/2$. In this case a little more than a quarter of the mean natural period T_{av} elapses between consecutive abrupt increases and decreases of the pendulum length. The graphs of the angle $\varphi(t)$ and angular velocity $\dot{\varphi}(t)$ for this periodic stationary process are shown in Fig. 10. We can write the corresponding time dependencies of $\varphi(t)$ and $\dot{\varphi}(t)$ for the time interval $(0, T/2)$ in the following form:

$$\varphi_1(t) = B_1 \sin \omega_1(t - T/4), \quad \dot{\varphi}_1(t) = B_1 \omega_1 \cos \omega_1(t - T/4), \quad 0 < t < T/2. \quad (23)$$

During the interval $(-T/2, 0)$ the graph in Fig. 10 is a segment of natural oscillation with the frequency $\omega_2 = \omega_0/\sqrt{1 - m}$:

$$\varphi_2(t) = -B_2 \cos \omega_2(t + T/4), \quad \dot{\varphi}_2(t) = B_2 \omega_2 \sin \omega_2(t + T/4), \quad -T/2 < t < 0. \quad (24)$$

Further calculations are similar to those for the left boundary described after Eqs. (15)–(16). It occurs that ΔT for the right boundary is determined as a solution to equation which differs from Eq. (22) by the opposite sign on its right-hand side. Solving it numerically by iterations

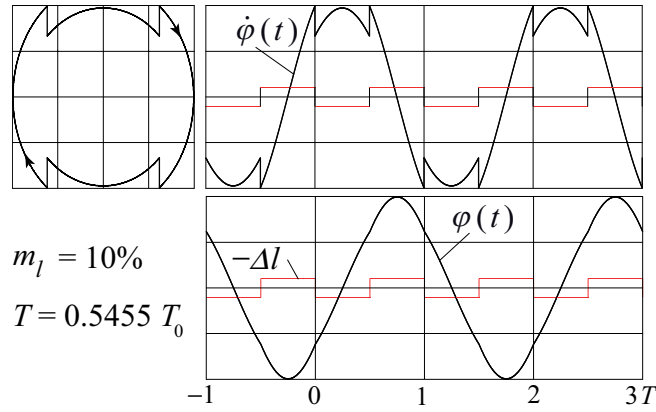


Figure 10: Stationary parametric oscillations at the upper boundary of the principal interval of instability (near $T = T_{\text{av}}/2$).

for various values of m_l , we obtain the right boundary of the principal interval ($n = 1$) of parametric instability, Fig. 9.

To obtain approximate analytical solutions to Eq. (22) that are valid for small values of the modulation depth m_l , we can simplify the expression on its right-hand side by assuming that $q \approx 1 + 3m_l$, $q - 1 \approx 3m_l$. We may also assume the value of the cosine to be approximately 1. On the left-hand side of Eq. (22), the sine can be replaced by its small argument, in which $\omega_{\text{av}} = 2\pi/T_{\text{av}}$. This yields the following approximate expressions for both boundaries of the main interval that are valid up to terms to the second order in m_l :

$$T_{\mp} = \frac{1}{2} \left(1 \mp \frac{3m_l}{\pi} \right) T_{\text{av}} = \frac{1}{2} \left(1 \mp \frac{3m_l}{\pi} - \frac{3m_l^2}{8} \right) T_0. \quad (25)$$

6.2. Third-order interval of parametric instability

The boundaries of the instability intervals that contain higher order parametric resonances can be determined in a similar way. At the third order resonance ($n = 3$) two cycles of variation of the pendulum length occur during approximately three natural periods of oscillation ($T \approx 3T_{\text{av}}/2$). The phase trajectories and the time-dependent graphs of stationary oscillations at the left and right boundaries of the third interval are shown in Fig. 11. The phase orbit of the periodic oscillation closes after two cycles of modulation. This orbit is formed by two concentric ellipses which correspond to small natural oscillations of the pendulum with frequencies ω_1 and ω_2 . The representative point moves clockwise along this orbit, jumping from one ellipse to the other each time the bob is shifted along the pendulum rod. The numbers in Fig. 11 make easier following how the representative point describes this orbit: equivalent points of the phase orbit and the graph of angular velocity are marked by equal numbers.

Considering conditions at which the graphs of natural oscillations with frequencies ω_1 and ω_2 on the left boundary fit one another for adjacent time intervals and produce the periodic process shown in Fig. 11, we get the same Eqs. (17)–(18) for A_1 and A_2 , as well as Eq. (22) for the period of modulation. Actually, this is true for all intervals of parametric instability of odd orders. Similarly, for the right boundary we get the same equations for B_1 and B_2 as in case $n = 1$, and also Eq. (22) with the opposite sign for determination of the corresponding period of modulation T . However, if we are interested in the third interval, we should search for a solution to these equations in the vicinity of $T = 3T_{\text{av}}/2$, as well as for any other interval of odd order n — in the vicinity of $T = nT_{\text{av}}/2$. The boundaries of intervals of the third and fifth orders, obtained by a numerical solution, are also shown in Fig. 9.

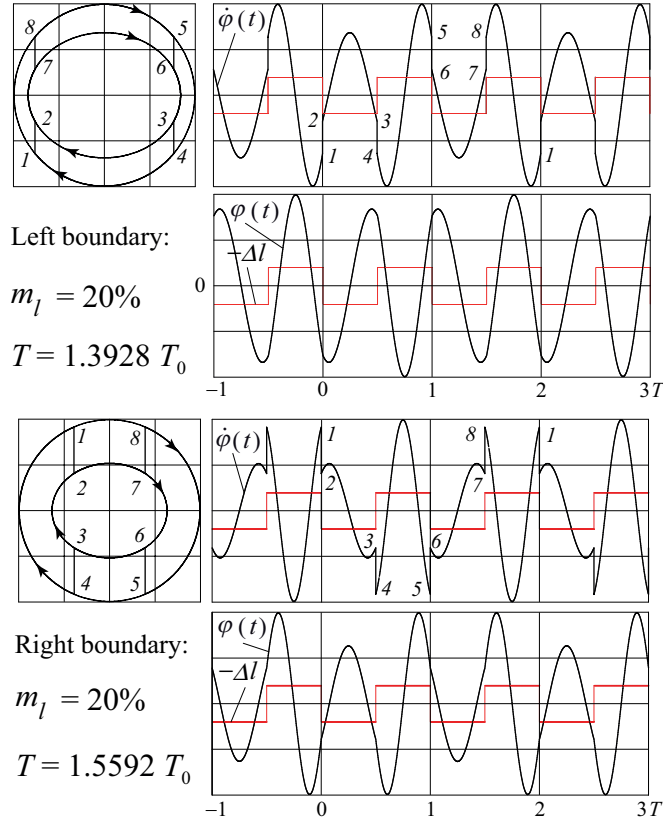


Figure 11: The phase trajectory and the graphs of the angular velocity and the deflection angle of stationary parametric oscillations at the left and right boundaries of the interval of instability near $T = 3T_{av}/2$.

For small values of the depth of modulation m_l , we can find approximate analytical expressions for the lower and the upper boundaries of the third interval that are valid up to quadratic terms in m_l :

$$T_{\mp} = \frac{3}{2} \left(1 \mp \frac{m_l}{\pi} \right) T_{av} = \frac{3}{2} \left(1 \mp \frac{m_l}{\pi} - \frac{3m_l^2}{8} \right) T_0, \quad m_l \ll 1. \quad (26)$$

In this approximation, the third interval has the same width $(3m_l/\pi)T_0$ as does the interval of instability in the vicinity of the principal resonance. However, this interval is distinguished by greater asymmetry: its central point is displaced to the left of the value $T = \frac{3}{2}T_0$ by $\frac{9}{16}m_l^2T_0$.

7. Parametric resonances of even orders

For small and moderate square-wave modulation of the pendulum length, parametric resonance of the order $n = 2$ (one cycle of the modulation during one natural period of oscillation) is relatively weak compared to the above considered resonances $n = 1$ and $n = 3$. In the case in which $n = 2$ the abrupt shifts of the bob induce both an increase and a decrease of the energy only once during each natural period. The growth of oscillations occurs only if the increase in energy at the instant when the bob is shifted up is greater than the decrease in energy when the bob is shifted down. This is possible only if the bob is shifted up when the angular velocity of the pendulum is greater in magnitude than it is when the bob is shifted down. For $T \approx T_{av}$, these conditions can fulfill only because there is a (small) difference between the natural periods T_1 and T_2 of the pendulum, where $T_1 = T_0\sqrt{1+m_l}$ is the period with the bob shifted down and

$T_2 = T_0\sqrt{1 - m_l}$ is the period with the bob shifted up. This difference in the natural periods is proportional to m_l .

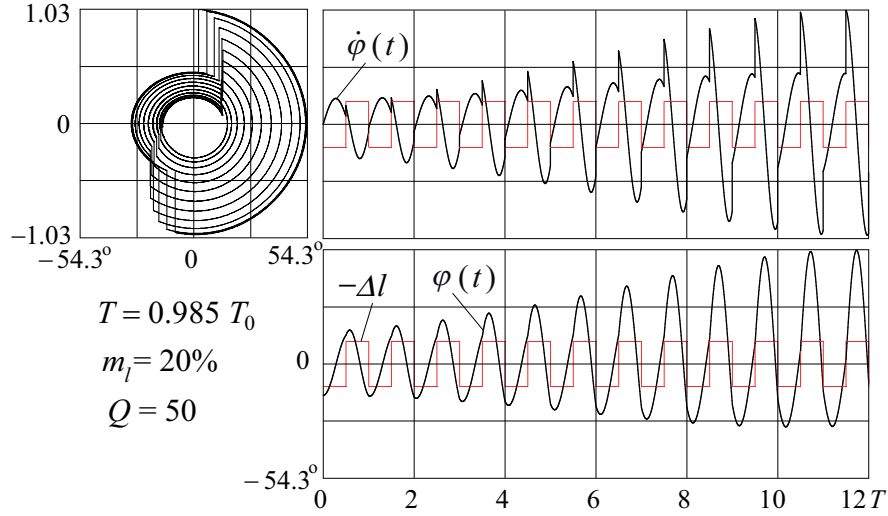


Figure 12: The phase trajectory and the graphs of angular velocity $\dot{\varphi}(t)$ and angle $\varphi(t)$ of oscillations corresponding to parametric resonance of the second order $n = 2$ ($T = T_{av}$).

The growth of oscillations at parametric resonance of the second order is shown in Fig. 12. We note the asymmetric character of oscillations at $n = 2$ resonance: the angular excursion of the pendulum to one side is greater than to the other. In this case, the investment in energy during a period is proportional to the *square* of the depth of modulation m_l , while in the cases of resonances with $n = 1$ and $n = 3$ the investment in energy is proportional to the first power of m_l . Therefore, for the same value of the damping constant γ (the same quality factor Q), a considerably greater depth of modulation is required here to exceed the threshold of parametric excitation. The growth of the amplitude again is restricted by the nonlinear properties of the pendulum.

The interval of instability in the vicinity of $n = 2$ resonance (for small values of m_l) is considerably narrower compared to the corresponding intervals of $n = 1$ and $n = 3$ resonances. Its width is also proportional only to the square of m_l .

To determine the boundaries of this interval of instability, we can consider, as is done above for other resonances, stationary oscillations for $T \approx T_0$ formed by alternating segments of free oscillations with the periods T_1 and T_2 . The phase trajectory and the graphs of the angular velocity $\dot{\varphi}(t)$ and the angle $\varphi(t)$ of such stationary periodic oscillations for one of the boundaries are shown in Fig. 13. During oscillations occurring at the boundary of the instability interval, the abrupt increment and decrement in the angular velocity exactly compensate each other.

To describe these stationary oscillations with small amplitude, we can use the following expressions for $\varphi(t)$ and $\dot{\varphi}(t)$ in the interval $(0, -T/2)$ (see Fig. 13):

$$\varphi_1(t) = -A_1 \cos \omega_1(t - T/4), \quad \dot{\varphi}_1(t) = A_1 \omega_1 \sin \omega_1(t - T/4), \quad 0 < t < T/2, \quad (27)$$

and during the interval $(-T/2, 0)$

$$\varphi_2(t) = A_2 \cos \omega_2(t + T/4), \quad \dot{\varphi}_2(t) = -A_2 \omega_2 \sin \omega_2(t + T/4), \quad -T/2 < t < 0. \quad (28)$$

The conditions for joining the graphs at $t = 0$ are the same as for other resonances, namely, at $t = 0$ we require $\varphi_1(0) = \varphi_2(0)$, and the angular velocity undergoes a sudden change, which

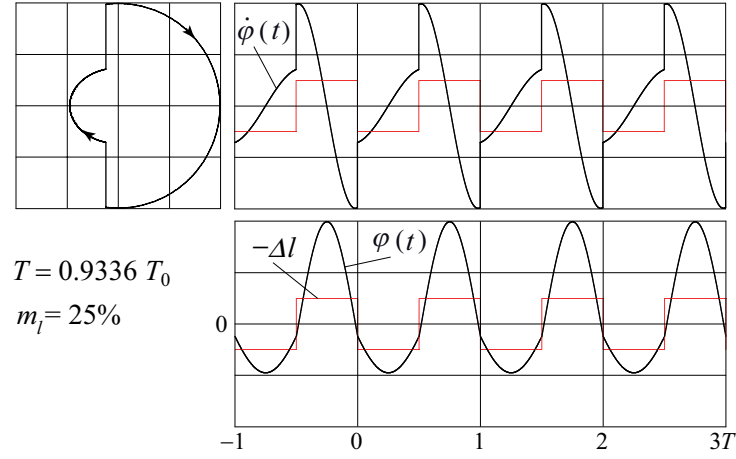


Figure 13: Stationary parametric oscillations at the left boundary of the interval of instability of the second order $n = 2$ (near $T = T_{\text{av}} \approx T_0$).

follows from the conservation of angular momentum (see Eq. (11)). From these conditions we find the following equations for A_1 and A_2 :

$$A_1 \cos(\omega_1 T/4) = -A_2 \cos(\omega_2 T/4), \quad (29)$$

$$A_1(1 + m_l)^2 \omega_1 \sin(\omega_1 T/4) = A_2(1 - m_l)^2 \omega_2 \sin(\omega_2 T/4). \quad (30)$$

These homogeneous equations (29)–(30) for A_1 and A_2 are compatible only if the following condition is fulfilled:

$$(1 + m_l)^2 \omega_1 \sin(\omega_1 T/4) \cos(\omega_2 T/4) = -(1 - m_l)^2 \omega_2 \sin(\omega_2 T/4) \cos(\omega_1 T/4). \quad (31)$$

This is the equation that determines period T of modulation (for a given value m_l of the depth of modulation) which corresponds to the left boundary of the 2nd interval of parametric instability. We transform Eq. (31) to the following form which is convenient for a numeric solution by iteration:

$$(q + 1) \sin(\omega_{\text{av}} T/2) = (q - 1) \sin(\Delta\omega T/4), \quad (32)$$

where q depends on the depth of modulation m_l according to Eq. (21). Next we replace T in the argument of the sine on the left-hand side of Eq. (32) by $T_{\text{av}} + \Delta T$. Since $\omega_{\text{av}} T_{\text{av}} = 2\pi$, we can write this sine as $-\sin(\omega_{\text{av}} \Delta T/2)$. Then Eq. (32) becomes:

$$\sin(\omega_{\text{av}} \Delta T/2) = -\frac{q - 1}{q + 1} \sin \frac{\Delta\omega(T_{\text{av}} + \Delta T)}{4}. \quad (33)$$

This equation for ΔT can be solved numerically by iteration with the help of the above described procedure. Its self-consistent solutions for various values of the modulation depth m_l give the left boundary of the $n = 2$ instability interval. After period T for this boundary is calculated, the initial conditions that provide stationary oscillations can be chosen on the basis of Eq. (27), according to which, for an arbitrary initial displacement $\varphi(0)$, the initial angular velocity should have the value $\dot{\varphi}_1(0) = \omega_1 \tan(\omega_1 T/4) \varphi_1(0)$.

The right boundary of the 2nd interval is given by equation which differs from Eq. (33) by the opposite sign on its right-hand side. Both boundaries are shown on the diagram in Fig. 9 together with intervals of higher even orders, which are obtained with the help of similar numeric calculations.

We note how the intervals of even resonances ($n = 2, 4, 6$) are narrow at small values of the modulation depth m_l in contrast to the intervals of odd orders. With the growth of m_l the even intervals expand and become comparable with the intervals of odd orders.

For small and moderate values of the depth of modulation $m_l \ll 1$, an approximate analytical expression for both boundaries of the 2nd interval of instability can be found as a solution to Eq. (33) (and to equation with the opposite sign for the other boundary):

$$T_{\mp} = \left(1 \mp \frac{3}{4}m_l^2\right) T_{\text{av}} = T_0 + \left(\mp \frac{3}{4} - \frac{3}{8}\right) m_l^2 T_0, \quad (34)$$

i.e., $T_- = T_0(1 - \frac{9}{8}m_l^2)$, $T_+ = T_0(1 + \frac{3}{8}m_l^2)$. As mentioned above, the width of this interval of instability $T_+ - T_- = \frac{3}{2}m_l^2 T_0$ is proportional to the square of the modulation depth.

8. Intersections of the boundaries at large modulation

Figure 9 shows that at certain values of m_l both boundaries of intervals with $n > 2$ coincide (we may consider that they intersect). This means that at these values of m_l the corresponding intervals of parametric instability disappear. Such values of m_l correspond to the natural periods of oscillation T_1 and T_2 , whose ratio is $2 : 1$, $3 : 1$, and $3 : 2$.

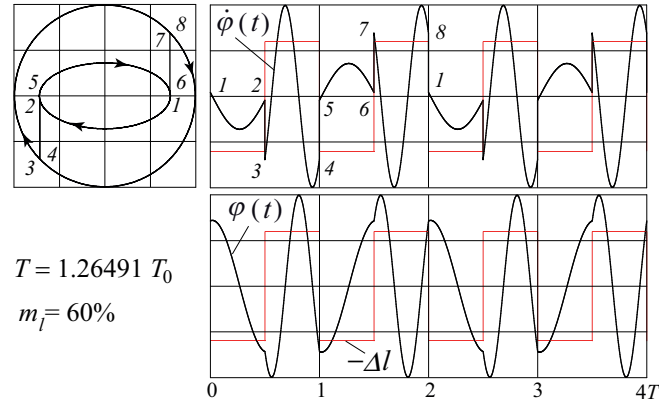


Figure 14: The phase trajectory and time-dependent graphs of angular velocity $\dot{\varphi}(t)$ and angle $\varphi(t)$ for stationary oscillations at the intersection of both boundaries of the third interval.

For the first intersection (ratio $2 : 1$) exactly one half of the natural oscillation with period T_1 is completed during the first half of the modulation cycle (see Fig. 14). On the phase diagram, the representing point traces a half of the smaller ellipse ($1 - 2$), and then abruptly jumps down to the larger ellipse ($2 - 3$). During the second half of the modulation cycle the oscillator executes exactly a whole natural oscillation with period $T_2 = T_1/2$, so that the representing point passes in the phase plane along the whole larger ellipse ($3 - 4$), and then jumps up to the smaller ellipse along the same vertical segment ($4 - 5$).

During the next modulation cycle the representing point generates first the other half of the smaller ellipse ($5 - 6$), and then again the whole larger ellipse ($7 - 8$). Therefore during any two adjacent cycles of modulation the representing point passes once along the closed smaller ellipse and twice along the larger one, returning finally to the initial point of the phase plane. We see that such an oscillation is periodic for arbitrary initial conditions. This means that for the corresponding values of the modulation depth m_l and the period of modulation T the growth of amplitude is impossible even in the absence of friction (the instability interval vanishes).

Similar explanations can be suggested for other cases in Fig. 9 in which the boundaries of the instability intervals intersect.

9. Intervals of parametric excitation in the presence of friction

When there is friction in the system, the intervals of the period of modulation that correspond to parametric instability become narrower, and for strong enough friction (below the threshold) the intervals disappear. Above the threshold, approximate values for the boundaries of the first interval are given by Eq. (25) provided we substitute for m_l the expression $\sqrt{m_l^2 - (m_l)_{\min}^2}$ with the threshold value $(m_l)_{\min} = \pi/(6Q)$ defined by Eq. (8). The proof can be found in Appendix. For the third interval, we can use Eq. (26), substituting $\sqrt{m_l^2 - (m_l)_{\min}^2}$ for m_l , with $(m_l)_{\min} = \pi/(2Q)$. When m_l is equal to the corresponding threshold value $(m_l)_{\min}$, the interval of parametric resonance disappears.

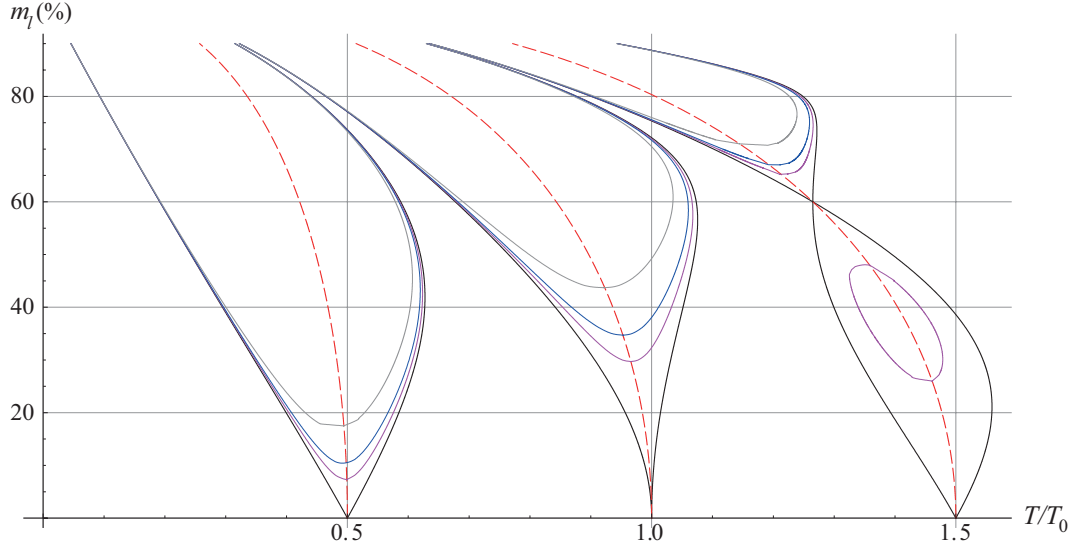


Figure 15: Intervals of parametric excitation at square-wave modulation of the pendulum length without friction, for $Q = 7$, $Q = 5$, and for $Q = 3$.

The boundaries of the second interval of parametric resonance in the presence of friction are approximately given by Eq. (34) provided we substitute for m_l^2 the expression $\sqrt{m_l^4 - (m_l)_{\min}^4}$ with the threshold value $(m_l)_{\min} = \sqrt{2/(3Q)}$, which corresponds to the second parametric resonance (see Appendix).

The diagram in Fig. 15 shows the boundaries of the first three intervals of parametric resonance for $Q = 3$, $Q = 5$, and $Q = 7$ (and also in the absence of friction). We note the “island” of parametric resonance of the 3rd order ($n = 3$) at $Q = 7$. This resonance disappears when the depth of modulation exceeds 48% and reappears when m_l exceeds approximately 66%.

In the presence of friction, for any given value m_l of the depth of modulation, only several first intervals of parametric resonance (where m_l exceeds the threshold) can exist. We note that in case the equilibrium of the system is unstable due to modulation of the parameter, parametric resonance can occur only if at least small oscillations are already excited. Indeed, when the initial values of φ and $\dot{\varphi}$ are exactly zero, they remain zero over the course of time. This behavior is in contrast to that of resonance arising from direct forcing, when the amplitude increases with time even if initially the system is at rest in the equilibrium position (if the initial conditions are zero).

10. Concluding remarks

We have shown in this paper that a pendulum whose length is subject to square-wave modulation by mass reconfiguration gives a very convenient example in which the phenomenon of

parametric resonance in a nonlinear system can be clearly explained physically with all its peculiarities. The threshold of parametric excitation is easily determined on the basis of energy considerations.

In a linear system, if the threshold of parametric excitation is exceeded, the amplitude of oscillations increases exponentially with time. In contrast to forced oscillations, linear viscous friction is unable to restrict the growth of the amplitude at parametric resonance. In real systems like the pendulum the growth of the amplitude is restricted by nonlinear effects that cause the natural period to depend on the amplitude. During parametric excitation the growth of the amplitude causes an increment in the natural period of the pendulum. The system slips out of resonance, the swing becomes smaller, and conditions of resonance restore. These transient beats fade out due to friction, and oscillations of finite amplitude eventually establish.

Computer simulations aid substantially in understanding the restriction of the amplitude growth over the threshold caused by nonlinear properties of the pendulum. The simulations illustrate the phenomenon of parametric autoresonance, stationary periodic oscillatory and rotational regimes that are possible due to the phase locking between the drive and the pendulum. The simulations reveal also bifurcations of symmetry breaking and intriguing sequences of period doubling. The boundaries of parametric instability for a pendulum with the square-wave modulated length are investigated quantitatively by rather modest mathematical means.

Appendix

The boundaries of instability in the presence of friction

Resonances of odd orders

Stationary oscillations occurring at the left boundary of the instability interval in the vicinity of the principal parametric resonance in the presence of friction are shown in Fig. 16 (compare with Fig. 8). Twice during the full cycle of modulation the angular velocity abruptly increases, and twice it decreases. The increments are greater than the decrements, so that as a whole the energy received by the pendulum exceeds the energy given away. This surplus compensates for the dissipation of the energy which occurs at natural oscillation during the intervals between the abrupt displacements of the bob along the rod of the pendulum.

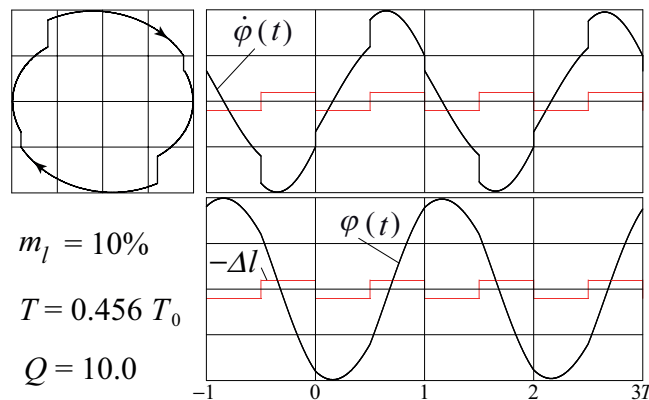


Figure 16: Stationary oscillations in the presence of friction at the left boundary of the principal instability interval.

To find conditions at which such stationary oscillations take place, we can write the expressions for $\varphi(t)$ and $\dot{\varphi}(t)$ during the adjacent intervals when the pendulum executes damped natural oscillations, and then fit these expressions to one another at the boundaries. Contrary to the frictionless pendulum (see Fig. 8), now the phase trajectory is not symmetric with respect to

the ordinate axis (Fig. 16). We choose as the time origin $t = 0$ the instant when the bob is shifted down, and the angular velocity decreases in magnitude. Then during the interval $(0, T/2)$ the graph describes a damped natural oscillation with the frequency $\omega_1 = \omega_0/\sqrt{1 + m_l}$. We can represent this motion as a superposition of damped oscillations of sine and cosine type with some constants A_1 and B_1 :

$$\begin{aligned}\varphi_1(t) &= (A_1 \sin \omega_1 t + B_1 \cos \omega_1 t) e^{-\gamma t}, \\ \dot{\varphi}_1(t) &\approx (A_1 \omega_1 \cos \omega_1 t - B_1 \omega_1 \sin \omega_1 t) e^{-\gamma t}.\end{aligned}\quad (35)$$

The latter expression for $\dot{\varphi}(t)$ is valid for relatively weak friction ($\gamma \ll \omega_0$). To obtain it, we differentiate $\varphi(t)$ with respect to the time, considering the exponential factor $e^{-\gamma t}$ to be approximately constant. Indeed, at weak damping the main contribution to the time derivative originates from the oscillating factors $\sin \omega_1 t$ and $\cos \omega_1 t$ in the expression for $\varphi(t)$. Similarly, during the interval $(-T/2, 0)$ the graph in Fig. 16 is a segment of damped natural oscillation with the frequency ω_2 :

$$\varphi_2(t) = (A_2 \sin \omega_2 t + B_2 \cos \omega_2 t) e^{-\gamma t}, \quad (36)$$

$$\dot{\varphi}_2(t) \approx (A_2 \omega_2 \cos \omega_2 t - B_2 \omega_2 \sin \omega_2 t) e^{-\gamma t}. \quad (37)$$

To determine the values of constants A_1 , A_2 , and B_1 , B_2 , we use the conditions that must be satisfied when the segments of the graph are joined together, and take into account the periodicity of the stationary process. At $t = 0$ the angle of deflection is the same for both φ_1 and φ_2 , that is, $\varphi_1(0) = \varphi_2(0)$. From this condition we get $B_2 = B_1$. We later denote these equal constants by B . The angular velocity at $t = 0$ undergoes a sudden change, which follows from the conservation of angular momentum: $(1 + m_l)^2 \dot{\varphi}_1 = (1 - m_l)^2 \dot{\varphi}_2$, see Eq. (11). This condition gives us the following relation between A_1 and A_2 : $A_2 = q A_1 = q A$ (further on we denote A_1 as A), where the factor q depends on modulation depth m_l according to Eq. (21).

For stationary periodic oscillations, corresponding to the principal resonance, as well as to all resonances of odd orders $n = 1, 3, \dots$ in Eq. (13), the conditions of periodicity are:

$$\varphi_1(T/2) = -\varphi_2(-T/2), \quad (1 + m)^2 \dot{\varphi}_1(T/2) = -(1 - m)^2 \dot{\varphi}_2(-T/2). \quad (38)$$

Substituting φ and $\dot{\varphi}$ in Eq. (38), we obtain the system of homogeneous equations for the unknown quantities A and B :

$$\begin{aligned}(p S_1 - q S_2) A + (p C_1 + C_2) B &= 0, \\ q(p C_1 + C_2) A - (p q S_1 - S_2) B &= 0,\end{aligned}\quad (39)$$

where $p = \exp(-\gamma T)$. In Eq. (39) the following notations are used:

$$\begin{aligned}C_1 &= \cos(\omega_1 T/2), & C_2 &= \cos(\omega_2 T/2), \\ S_1 &= \sin(\omega_1 T/2), & S_2 &= \sin(\omega_2 T/2).\end{aligned}\quad (40)$$

The homogeneous system of Eqs. (39) for A and B has a non-trivial (non-zero) solution only if its determinant is zero:

$$2q C_1 C_2 - (1 + q^2) S_1 S_2 + q(p + 1/p) = 0. \quad (41)$$

This condition for the existence of a non-zero solution to Eqs. (39) gives us an equation for the unknown variable T , which enters Eq. (41) as the arguments of sine and cosine functions in S_1 , S_2 and C_1 , C_2 , and also as the argument of the exponent in $p = e^{-\gamma T}$. The desired boundaries of

the interval of instability T_- and T_+ are given by the roots of the Eq. (41). To find approximate solutions T to this transcendental equation, we transform it into a more convenient form. We first represent in Eq. (41) the products C_1C_2 and S_1S_2 as follows:

$$C_1C_2 = \frac{1}{2}\left(\cos \frac{\Delta\omega T}{2} + \cos \omega_{\text{av}}T\right), \quad S_1S_2 = \frac{1}{2}\left(\cos \frac{\Delta\omega T}{2} - \cos \omega_{\text{av}}T\right), \quad (42)$$

Then, using the identity $\cos \alpha = 2 \cos^2(\alpha/2) - 1$, we reduce equation (41) to the following form:

$$(q + 1) \cos(\omega_{\text{av}}T/2) = \pm \sqrt{(q - 1)^2 \cos^2(\Delta\omega T/4) - q(p + 1/p - 2)}. \quad (43)$$

To find the boundaries of the interval which contains the principal resonance, we should search for a solution T of Eq. (43) in the vicinity of $T = T_0/2 \approx T_{\text{av}}/2$. If for a given value of the quality factor Q (Q enters $p = e^{-\gamma T}$) the depth of modulation m_l exceeds the threshold value, Eq. (43) has two solutions which correspond to the desirable boundaries T_- and T_+ of the instability interval. These solutions exist if the expression under the radical sign in Eq. (43) is positive. Its zero value corresponds to the threshold conditions:

$$\frac{(q - 1)^2}{q} \cos^2(\Delta\omega T/4) = p + \frac{1}{p} - 2. \quad (44)$$

To evaluate the threshold value of Q for small values of the modulation depth $m_l \ll 1$, we may assume here $q \approx 1 + 3m_l$ (see Eq. (21)), and $\cos(\Delta\omega T/4) \approx 1$. On the right-hand side of Eq. (44), in $p = e^{-\gamma T}$, we can consider $\gamma T \approx \gamma T_0/2 = \pi/(2Q) \ll 1$, so that $p + 1/p - 2 \approx (\gamma T)^2 = (\pi/2Q)^2$. Thus, for the threshold of the principal parametric resonance we obtain

$$Q_{\min} \approx \frac{\pi}{6m_l} \quad (m_l)_{\min} \approx \frac{\pi}{6Q}. \quad (45)$$

At the threshold the expression under the radical sign in Eq. (43) is zero. Both its roots (the boundaries of the instability interval) merge. This occurs when the cosine on the left-hand side of Eq. (43) is zero, that is, when its argument equals $\pi/2$:

$$\omega_{\text{av}} \frac{T}{2} = \frac{\pi}{2}, \quad \text{or} \quad T = \frac{\pi}{\omega_{\text{av}}} = \frac{1}{2}T_{\text{av}},$$

so that the threshold conditions (45) correspond to exact tuning to resonance, when $T = T_{\text{av}}/2$.

To find the boundaries T_- and T_+ of the instability interval, we represent T in the argument of the cosine function on the left-hand side of Eq. (43) as $T_{\text{av}}/2 + \Delta T$. Since $\omega_{\text{av}}T_{\text{av}} = 2\pi$, we can write this cosine as $-\sin(\omega_{\text{av}}\Delta T/2)$. Then Eq. (43) becomes:

$$\sin(\omega_{\text{av}}\Delta T/2) = \mp \frac{1}{q + 1} \sqrt{(q - 1)^2 \cos^2 \frac{\Delta\omega(\frac{1}{2}T_{\text{av}} + \Delta T)}{4} - q \frac{(p - 1)^2}{p}}. \quad (46)$$

For zero friction $p = 1$, and Eq. (46) coincides with Eq. (21). The diagram in Fig. 15 is obtained by numerically solving this equation for ΔT by iteration. Boundaries of the instability for intervals of higher odd orders $n = 3, 5, \dots$ are calculated similarly by representing T in Eq.(43) as $nT_{\text{av}}/2 + \Delta T$. They are also shown in Fig. 15 for several values of the quality factor Q . For large values of the modulation depth m_l these boundaries almost merge with the corresponding boundaries in the absence of friction.

To find an approximate solution of Eq. (46), that is valid for small values of the modulation depth $m_l \ll 1$ up to terms to the second order in m_l , we can simplify the expression under the radical sign on the right-hand side of Eq. (39), assuming $q \approx 1 + 3m_l$, $(q - 1)^2 \approx 9m_l^2$, and

the value of the cosine function to be 1. The last term of the radicand can be represented as $(\pi/6Q)^2 \approx (m_l)_{\min}^2$. On the left-hand side the sine can be replaced with its small argument, where $\omega_{\text{av}} = 2\pi/T_{\text{av}}$. Thus we obtain:

$$\frac{\Delta T}{T_{\text{av}}} \approx \mp \frac{3}{2\pi} \sqrt{m_l^2 - (m_l)_{\min}^2}, \text{ or } T_{\mp} = \frac{T_{\text{av}}}{2} \left(1 \mp \frac{3}{\pi} \sqrt{m_l^2 - (m_l)_{\min}^2} \right). \quad (47)$$

For the case of zero friction $(m_l)_{\min} = 0$, and these approximate expressions for the boundaries of the instability interval reduce to Eq. (25). For the threshold conditions $m_l = (m_l)_{\min}$, and both boundaries of the interval merge, that is, the interval disappears.

After the substitution of one of the roots T_- or T_+ of Eq. (25) into (39), both equations for A and B become equivalent and allow us to find only the ratio A/B . Nevertheless, these oscillations have a definite shape which is determined by the ratio of the amplitudes A and B of the sine and cosine functions whose segments form the pattern of the stationary parametric oscillation (see Figs. 8 and 10).

Resonances of even orders

To describe stationary oscillations occurring on the boundaries of instability intervals of even orders, we can use the same expressions for $\varphi(t)$ and $\dot{\varphi}(t)$, Eqs. (35) and (37). The conditions of joining the graphs at $t = 0$ are also the same. However, the conditions of periodicity at the instants $-T/2$ and $T/2$ for resonances of even orders differ from Eqs. (38) by the opposite sign. This yields, instead of Eq. (43), the following equation for the boundaries of instability intervals:

$$(q + 1) \sin(\omega_{\text{av}}T/2) = \pm \sqrt{(q - 1)^2 \sin^2(\Delta\omega T/4) - q(p + 1/p - 2)}. \quad (48)$$

For the interval of the 2nd order, we should search for its solution T in the vicinity of $T_0 \approx T_{\text{av}}$. If for a given value of the quality factor Q (Q enters $p = e^{-\gamma T}$) the depth of modulation m_l exceeds the threshold value, Eq. (48) has two solutions which correspond to the boundaries T_- and T_+ of the instability interval. These solutions exist if the expression under the radical sign in Eq. (48) is positive. Its zero value corresponds to the threshold conditions, that is, to $(m_l)_{\min}$ for a given Q or Q_{\min} for a given m_l :

$$\frac{(q - 1)^2}{q} \sin^2(\Delta\omega T_{\text{av}}/4) = \frac{(p - 1)^2}{p}. \quad (49)$$

The threshold conditions fulfil at exact tuning to 2nd resonance, when $T = T_{\text{av}}$. To estimate the threshold value of Q for small values of the modulation depth m_l , we may assume here $q \approx 1 + 3m_l$, $\sin(\Delta\omega T/4) \approx \Delta\omega T_0/4$, and $\Delta\omega \approx m_l\omega_0$. On the right-hand side of Eq. (49), in $p = e^{-\gamma T}$, we can consider $\gamma T \approx \gamma T_0 = \pi/Q \ll 1$, so that $p + 1/p - 2 = (p - 1)^2/p \approx (\gamma T)^2 = (\pi/Q)^2$. Thus, for the threshold of the 2nd parametric resonance we obtain:

$$Q_{\min} \approx \frac{2}{3m_l^2}, \quad (m_l)_{\min} \approx \sqrt{\frac{2}{3Q}}. \quad (50)$$

To find the boundaries T_- and T_+ of the 2nd instability interval, we represent T in the argument of the sine function on the left-hand side of Eq. (48) as $T_{\text{av}} + \Delta T$. Since $\omega_{\text{av}}T_{\text{av}} = 2\pi$, we can write this sine as $-\sin(\omega_{\text{av}}\Delta T/2)$. Then Eq. (48) becomes:

$$\sin \frac{\omega_{\text{av}}\Delta T}{2} = \mp \frac{1}{q + 1} \sqrt{(q - 1)^2 \sin^2 \frac{\Delta\omega(T_{\text{av}} + \Delta T)}{4} - q \frac{(p - 1)^2}{p}}. \quad (51)$$

This form of the equation is convenient for numerical solution by iteration. For the zero friction $p = 1$, and Eq. (51) coincides with Eq. (33). To obtain an approximate solution to Eq. (51), valid for small values of the modulation depth m_l up to the terms of the second order of m_l , we can simplify the expression under the radical sign on the right-hand side of Eq. (51), assuming $q \approx 1 + 3m_l$, $(q - 1)^2 \approx (3m_l)^2$, and $\sin[\Delta\omega(T_{av} + \Delta T)/4] \approx \Delta\omega T_{av}/4 = \pi m_l/2$. The last term of the radicand can be represented as $(2/3Q)^2 \approx (m_l)_{\min}^4$. On the left-hand side the sine can be replaced by its small argument, where $\omega_{av} = 2\pi/T_{av}$. Thus for the boundaries of the second instability interval we get:

$$\frac{\Delta T}{T_{av}} \approx \mp \frac{3}{4} \sqrt{m_l^4 - (m_l)_{\min}^4}, \quad \text{or} \quad T_{\mp} = \left(1 \mp \frac{3}{4} \sqrt{m_l^4 - (m_l)_{\min}^4} \right) T_{av}. \quad (52)$$

References

- [1] H. W. Broer, I. Hoveijn, M. van Noort, C. Simó, G. Vegter, The Parametrically Forced Pendulum: A Case Study in $1\frac{1}{2}$ Degree of Freedom, *J. Dynamics and Differential Equations*, **16** (2004) 897–947.
- [2] E. I. Butikov, On the dynamic stabilization of an inverted pendulum, *Am. J. Phys.* **69** (2001) 755–768.
- [3] E. I. Butikov, Subharmonic Resonances of the Parametrically Driven Pendulum, *J. Phys. A: Math. and Gen.* **35** (2002) 6209–6231.
- [4] E. I. Butikov, Regular and Chaotic Motions of the Parametrically Forced Pendulum: Theory and Simulations, in: *Computational Science – ICCS 2002* (Springer Verlag, 2002, LNCS 2331, 2009, pp. 1154–1169).
- [5] E. I. Butikov, An improved criterion for Kapitza’s pendulum stability, *J. Phys. A: Math. and Theor.* **44** (2011), 295202 (16 pp).
- [6] S. M. Curry, How children swing, *Am. J. Phys.* **44** (1976) 924–926.
- [7] P.L. Tea Jr., H.Falk, Pumping on a swing, *Am. J. Phys.* **36** (1968) 1165–1166 .
- [8] W. Case, The pumping of a swing from the standing position, *Am. J. Phys.* **64** (1996) 215–220.
- [9] M. A. Pinsky, A. A. Zevin, Oscillations of a pendulum with a periodically varying length and a model of swing, *Int. J. Non-Linear Mech.* **34** (1999) 105–109.
- [10] D. Stilling, W. Szyskowski, Controlling angular oscillations through mass reconfiguration: a variable length pendulum case, *Int. J. Non-Linear Mech.* **37** (2002) 89–99.
- [11] G. L. Baker, J. A. Blackburn, *The Pendulum: A Case Study in Physics*, Oxford University Press, 2005.
- [12] E. I. Butikov, Pendulum with a square-wave modulated length (simulation program), <http://faculty.ifmo.ru/butikov/Applets/PendParSquare.html>
- [13] E. I. Butikov, Parametric resonance, *Comput. Sci. Eng.* (1999) 76–83.
- [14] E. I. Butikov, Parametric excitation of a linear oscillator, *Eur. J. Phys.* **25** (2004) 535–554.
- [15] E. I. Butikov, Parametric resonance in a linear oscillator at square-wave modulation, *Eur. J. Phys.* **26** (2005) 157–174.